Lattice layout and linear optics for sharing superconducting linac

Miho Shimada

High Energy Accelerator Research Organization, KEK, Oho 1-1, Tsukuba, Ibaraki, 305-0801, Japan

(Received 19 September 2018; published 11 April 2019)

A superconducting (SC) linac allows a few orders of magnitude larger average beam current than a normal conducting linac, therefore the powerful beam is expected to lead to outstanding discoveries in various scientific fields, such as high luminosity accelerators and high brilliance light source. However, the high construction and operation costs of the SC linac is a critical issue for realizing large scale facilities. To resolve this problem, we propose a continuous wave (cw) operation of an SC linac shared by electron/positron beams for effective multipurpose utilization. A high current positron source is required for high-energy physics projects: a linear electron-positron collider and a muon collider, while high-current and high-quality electron beams are expected to realize the high brilliant x-ray light sources. As an example, we discuss the injector of the International Linear Collider, an x-ray free-electron laser, and an energy-recovery linac light source. We found a feasible solution of a basic design for the proposed multibeam operation despite the high-quality beam requirements and complicated operation: control of mixed beams without pulsed magnets, and heat load in the cavity, high stability of beam energy, and operation at high average current.

DOI: 10.1103/PhysRevAccelBeams.22.041602

I. INTRODUCTION

As the surface of a superconducting (SC) accelerator cavity has an extremely small resistance, high accelerating rf fields can be applied with little heating. Consequently, the long-pulse or continuous-wave (cw) operation enables us to increase beam repetition rate, and the cost performance per beam current is the highest among linear accelerators such as normal-conductivity cavities, and laser-based accelerators. This technique is therefore expected in state-of-the-art large-scale linear accelerators for projects in high-energy particle physics, photon science, and neutron science and applications [1–4]. Some of these projects utilize the 1.3 GHz TESLA nine-cell cavity developed under the International Linear Collider (ILC) project [1], an electron-positron collider aiming at the collision energy of 500 GeV. Although it is developed for 1 ms pulse operation, cw operation is possible at the relatively lower acceleration gradient. It is expected to be applied in several fields because it allows the longer pulse operation.

As one example, future linear collider projects such as the ILC and the Compact Linear Collider (CLIC) [5] require high-current positron sources with a flux of $10^{14–15}e+/s$, which is several orders of magnitude larger than the existing positron source. In addition, the much higher positron flux is necessary for muon colliders [6,7]. Such a high current positron beam is generated by driving electrons or gamma rays towards a metal target with a large atomic number. Among the most serious technical problems is the thermal loading of the positron target. The operation with longer pulses is expected to reduce the peak current and mitigates the thermal loading. In the baseline scheme of the ILC, positron source is based on gamma rays from a helical undulator driven by 150 GeV electron beam. Because of the high operation cost of the high-energy electron beam, the pulse duration is limited to 1 ms. Therefore, several other positron sources driven by a lower energy electron beam are proposed. Some of them are based on gamma rays by the inverse Compton scattering with lower electron beams, which is potentially realized through the SC linac in cw operation by a technique of energy recovery [8,9]. Another is called a conventional method, directly driving electron beams toward the target [10,11]. The conventional method is considered as the backup scheme because the required energy of the drive electrons is only a few GeV and it enables the long pulse operation at a reasonable operation cost for reducing the thermal loading. The long-pulse structure of the positrons is be converted to 1 ms pulses at the damping ring (DR) before injection into the main linac as shown in Fig. 1.

As the current backup scheme of the positron source of the ILC is based on an normal conducting (NC) linac, the long pulse consists of thousands of micropulses (duration 1 μs) at 300 Hz to avoid heating by rf fields. Owing to the

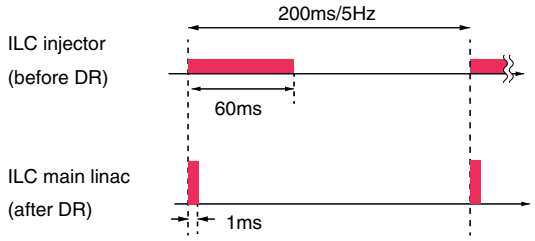

FIG. 1. The schematic of the pulses before/after the main linac of the ILC. The pulse length of the ILC injector is much longer than that of the main linac of the ILC to reduce the thermal loading at the backup scheme.

complicated pulse structure, two individual GeV-class NC linacs are required to accelerate the drive electrons for the target and the positrons for injection into the 5 GeV DR. The high peak current of the micropulse causes another problem such as a shock wave on the target and beam loading of the accelerator linacs. Therefore, we proposed to utilize an SC linac instead of the current backup scheme. The SC linac makes it possible to operate at a long pulse without micropulses, therefore it is expected to more mitigate the problems as well as the thermal loading problem. In addition, the SC linac can also accelerate the polarized electrons for the ILC collision experiment at the same bunch pattern. The three beams are collectively called the "ILC injector." In our proposal, the three beams (polarized electrons, positrons and drive electrons) share a 6–7 GeV SC injector linac. The schematic is shown in Fig. 2.

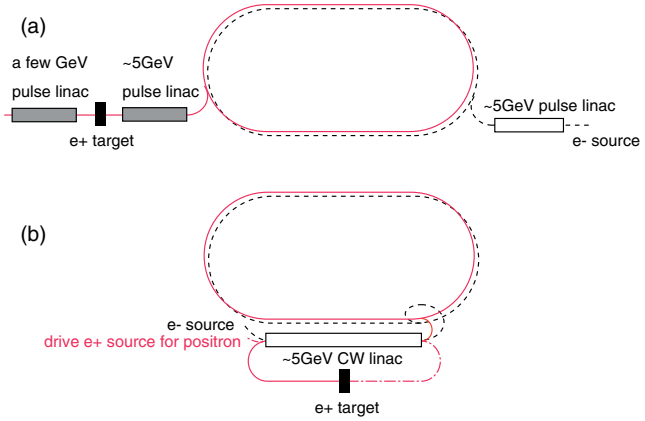

FIG. 2. Layouts of the ILC injector based on the electron driven (conventional) positron source based on (a) a normal conducting linac and (b) a cw superconducting linac.

The SC linac is also a promising facility to realize x-ray light sources with high flux and brilliance owing to the high electron beam current. The European X-ray Free-Electron Laser (XFEL) at DESY [2] has successfully generated the first x-ray laser with an SC linac. Subsequently, SLAC started the LCLS-II XFEL project [3], which will operate the SC linac in cw mode. As an x-ray source with exceptional brightness, XFEL with an oscillator is also proposed [12]. Alternatively, one of the candidates of the next-generation x-ray light source is an ERL composed of an SC linac and a recirculation loop [13–15]. Because the recirculating beam returns its beam energy to the linac, the average beam current is much higher than a linac without energy recovery. It also makes it possible to transport the high-quality beam and utilize its high brilliant light source. The km-scale recirculation loop of an ERL provides 20–30 beam lines, whereas the XFEL provides only a few beam lines. Some sub-GeV class ERLs have already been demonstrated and are under construction at several laboratories [15–18].

However, the huge construction and operation costs of the SC linac are critical issues. To reduce these costs, several projects accelerate the electron beam multiple times through the SC linac [19–22]. In this article, we propose another approach: effective use of an SC linac by sharing of multipurpose tasks. As one example, we apply an electron/positron multibeam as the injector of the ILC, XFEL and ERL light source (ERL-LS) with little degradation of the source performances [23,24]. The multibeam injection has been already proven successful at SLAC Linear Collider, SLC and the injector for the storage rings of the KEKB accelerator and the Photon Factory [25,26]. In addition, a superconducting linac at TRIUMF also has a plan to share the electron beam for ARIEL target and FEL-ERL [27]. However, several features that are not required in these multibeam operations may be crucial in this proposed scheme. These features include control of mixed beams without pulsed magnets, heat load in the superconducting cavity, high stability of beam energy, operation at high average current (larger than 10 mA), and bunch compression to sub-ps bunch length.

II. LAYOUT OF ACCELERATOR

The layout of our proposal for the ILC injector is shown in Fig. 3. The 6–7 GeV linac is divided into a short and long linac. First, the drive electrons are accelerated sufficiently to hit the positron target. Because the positron just emitted

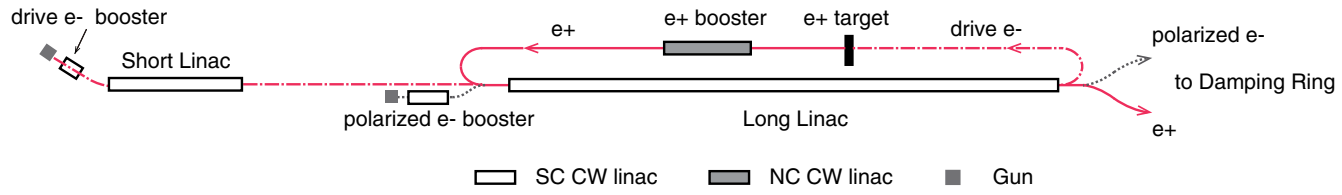

FIG. 3. Schematic of the proposed layout for the ILC injector with positrons, drive electrons, and polarized electrons.

TABLE I. Beam energies at the entrance to the short linac ($E_{\mathrm{in}}^{\mathrm{short}}$), long linac ($E_{\mathrm{in}}^{\mathrm{long}}$), and at the exit from the long linac ($E_{\mathrm{out}}^{\mathrm{long}}$). The electrons for XFEL in the short linac and the drive electrons in both linacs are accelerated at an off-crest phase.

	$E_{\mathrm{in}}^{\mathrm{short}}$ [MeV]	$E_{\mathrm{in}}^{\mathrm{long}}$ [GeV]	$E_{\mathrm{out}}^{\mathrm{long}}$ [GeV]
XFEL	500	2.4	7
ERL-LS(acc)	30	1.9	6.5
ERL-LS(dec)	1900	6.5	1.9
Drive e−	∼30	1.7	5.7
e+	⋯	0.4	5
Polarized e−	⋯	0.4	5

from the target is low quality and accompanied by other radiation particles emitted from the target, it is accelerated by the NC booster to nearly 400 MeV and collimated before injection into the long SC linac to avoid breaking the superconductivity. The beam optics of the long SC linac are optimized such that the transverse size of the positron beam remains much smaller than the iris radius of the accelerating cavity (35 mm), even during multibeam operation. For easy beam operation, the polarized electrons and positrons are injected at the same energy, while the drive electrons are injected at higher energy. The energy of each electron beam differs at the end of the SC linac (see Table I), so the orbits of the three beams can be separated without pulsed magnets. The NC booster should be operated in long pulse or cw mode, but the frequency can be other than 1.3 GHz. In the Very High Frequency (VHF) region (∼180 MHz), long period cw operation has been demonstrated in an NC linac [28].

The SC linac has sufficient capacity to furnish high-brilliance x-ray light sources because the ILC requires only a low average current (less than a few hundred μA) and a blank interval exceeding 100 ms at 5 Hz for the damping time. As the light source, we consider both XFEL and ERL-LS. The XFEL provides a high-brilliance, large-flux light source whereas the ERL-LS enables a large number of beam lines. The layout of the XFEL and ERL-LS is shown in Fig. 4. The two SC linacs are consistent with Fig. 3. The beam energies at the entrances and exits of the linacs differ by at least 10% (see Table I). The energy gain depends on the accelerating phase. The chicane located between the long and short linac enables individual control of the orbit and optics of each beam. Bunch compression of the electrons for XFEL [2] can then be accomplished, by energy chirp induced by off-crest acceleration and nonzero longitudinal dispersion through the chicanes.

III. BEAM PARAMETERS

A. Beam energy and current

An ERL-booster linac accelerates the electron beam up to the short linac injection energy $E_{\mathrm{in}}^{\mathrm{short}}$, and the return electron beam is decelerated at the two SC linacs and transported into the dump line as shown in Fig. 4. For the ERL-LS, the design value of the average electron beam current is a few 10 mA, which is limited in the threshold current due to beam breakup caused by higher order modes (HOM-BBU) [29–33]. In order to increase the threshold current, the ERL-booster energy is designed to a few 10 MeV, which is larger than the other ERL projects [13,14]. The power consumption of the booster also limits the booster energy because it is operated without energy recovery. On the other hand, the average current for the XFEL is limited to a few 100 μA to prevent radiation hazard at the beam dump. In addition, the heat load due to the beam transport in the 2 K region should be careful because it becomes larger at the high current and the shorter bunch length operation [34,35]. It is assumed to be approximately 10 W at the long linac, in which the bunch length for XFEL beams is fully compressed, as shown in Table II. The main beam parameters are also summarized in Table II.

B. Bunch structure and pattern

In the same manner with the backup scheme, the pulse duration of the proposed ILC injector is assumed to be the 60 ms (see Fig. 1). Moreover, the bunch repetition rate is maintained constant at 50 kHz, corresponding to 1 ms pulses at 3 MHz in the main linac of the ILC. The long pulses of the positrons and polarized electrons should be overlapped to match the collision timing of the ILC experiments. On the other hand, the positrons are assumed to trail the drive electrons by 5–6 μs because they turn around after the almost 700 m-long linac, the positron target, and the NC linac (see Fig. 3). For simplicity, the polarized electrons are injected behind the positrons with the same delay time. The pulse and bunch structure of the electron/positron beams are shown in panels (a) and (c) of Fig. 5, respectively. Hereafter these three pulses are collectively termed the "ILC pulse."

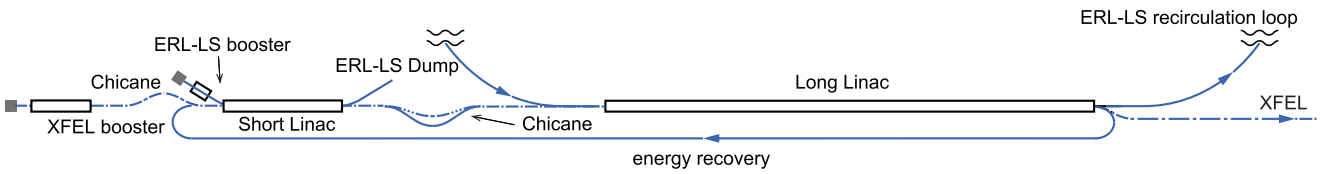

FIG. 4. Schematic of the proposed layout of the XFEL and ERL light sources. Two chicanes are located between the linacs for individual control of each beam.

TABLE II. Main beam parameters and heat load power in the long linac. Energy recovery (ER) is the summed current of the accelerated and decelerated beams.

	ε_n [m · rad]	q [nC]	σ_z [mm]	I [mA]	Heat load [W/m]
XFEL	1×10^{-6}	0.3	0.02	0.1	1
ERL-LS	1×10^{-7}	0.01	0.3	20 (ER)	5
Drive e−	1×10^{-4}	3	A few	0.05	<1
e+	1×10^{-2}	3	A few	0.05	<1
Polarized e−	1×10^{-4}	3	A few	0.05	<1

The bunch charge of 3 nC in the ILC causes beam loading, which (according to rough estimate) induces $O(0.1\%)$ fluctuations of the accelerating field in the cavity [36,37]. An example of the accelerator gradient is shown in Fig. 6. These fluctuations induce correlated electron fluctuations at a much higher repetition rate (a few MHz or 1.3 GHz for x-ray sources). As the electron energy stability of an x-ray light source must be better than 0.01% the electrons for the light source are operated in the 140-ms blank interval between the ILC pulses to avoid beam loading. In the same way, beam loading of a few hundred pC per bunch in the XFEL induces non-negligible energy fluctuations of the electrons for the ERL-LS. Therefore, the three pulses—ILC, XFEL, and ERL-LS—must never overlap, as shown in Figs. 5(a) and 5(b). The blank interval time between the three pulses is larger than the time constant of the accelerating cavity (which is of the order of a few ms), sufficient for stabilization of the accelerating field by feedback systems.

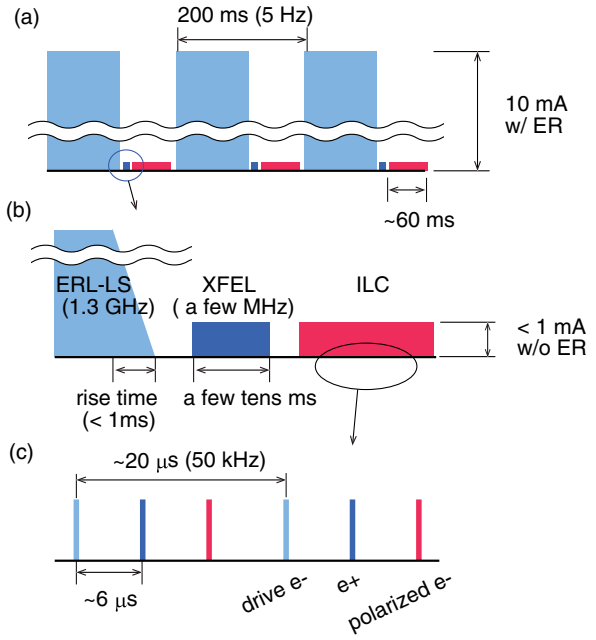

FIG. 5. Example of the bunch and pulse structure of the electron/positron beams for the ILC, XFEL, and ERL-LS.

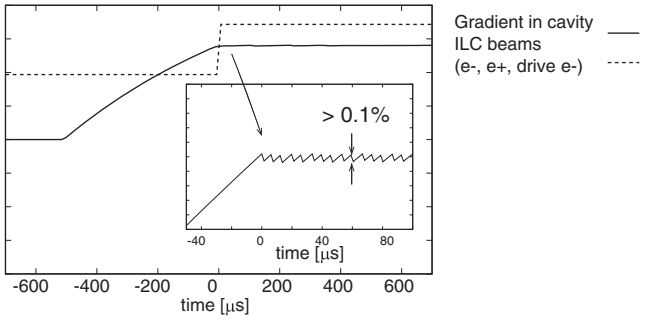

FIG. 6. Fluctuation of the accelerator gradient in the cavity caused by the beam loading of the 3 nC ILC beam.

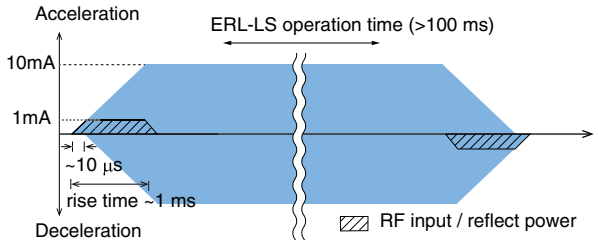

FIG. 7. Power exchange between the electron beam and rf power supply during long pulse operation of ERL-LS at high average current (~10 mA).

In long-pulse operation, the beams must be accelerated without energy recovery (ER) until the head of the electron beam pulse returns from the recirculation loop. For this reason, the average current of the pulse for the ERL-LS gradually increases during part of the rise time [Fig. 5(b)]. Figure 7 shows the power exchange of the energy between the electron beam and the rf power supply. The return of the current pulse from the km-scale recirculation loop is assumed to consume almost 10 μs. SC linacs are designed to accelerate the average electron beam current from 100 μA to 1 mA without ER. Therefore the rise time was selected almost 1 ms. On the other hand, ER is unnecessary for the ILC and XFEL because of the low average beam current.

Each beam can be accelerated or decelerated at a phase optimized for each beam. The ILC beams are accelerated in slightly off-crest phase to minimize the effect of the internal wakefield caused by the 3 nC bunch charge, and the electrons for the XFEL are mainly optimized for bunch compression as mentioned above. Meanwhile, the electrons for the ERL-LS should be a perfectly on-crest acceleration to minimize the energy spread induced by the 1.3 GHz rf curve.

IV. LINEAR OPTICS DESIGN

The energy of each beam differs along the two linacs, as shown in Fig. 8. The accelerating gradient of the SC linac is assumed as 15 MV/m at the cw operation. The full

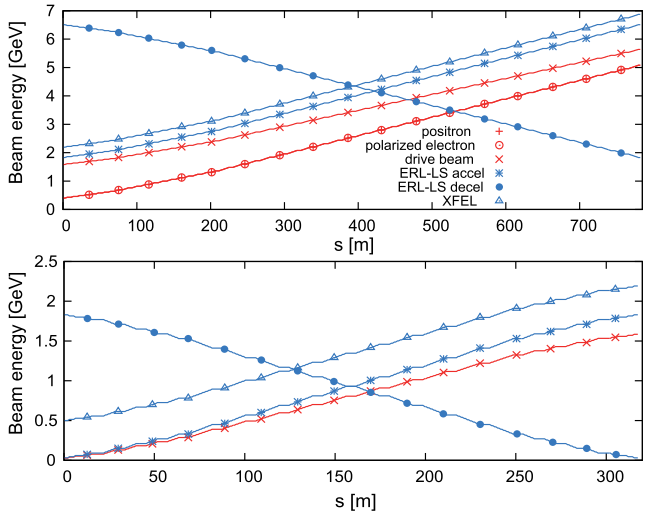

FIG. 8. Energies of the various beams along the long linac (upper panel) and short linac (bottom panel). Note that the energies of the positrons and polarized electron beam overlap.

accelerations in the long and short linacs are 4.6 GeV and 1.9 GeV, respectively. The beam-focusing system consists of quadrupole triplets inserted between the SC accelerating cavities. The focusing strength of each quadrupole magnet is inversely proportional to the beam energy. The root-mean-square (rms) transverse beam size $\sigma_{x,y}$ is described by the normalized emittance $\varepsilon_{x,y}$ and Lorentz factor γ as $\sigma_{x,y} = \sqrt{\beta_{x,y}\varepsilon_{x,y}/\gamma}$, where $\varepsilon_{x,y}$ is invariable for each beam. Under this condition, the entire beam optics for transporting the beams at a reasonable transverse size and betatron function are determined by the following strategies.

The linacs are mainly composed of superconducting accelerator cavities stored in cryostat modules and quadrupole magnets located at the normal temperature region. As shown in Table II, the positron beams have extremely large emittance before entering the DR, therefore the linear optics should be optimized for positron beam so that the rms transverse sizes in the cavity, $\sigma_{x,y}$, are maintained much smaller than the iris radius of the accelerating cavity r, e.g., $5\sigma_{x,y} < r$. In order to effectively remove the widely spread beam tail and halo in both directions of x and y, the polarities of the quadrupole triplets, focus-defocus-focus and defocus-focus-defocus, are settled alternately at the normal temperature region.

In addition, the entire betatron function of ERL-LS beams should be suppressed to increase the threshold beam current due to the HOM-BBU. It is challenging because several beams at different energy pass through the linacs. The betatron functions are optimized for the lowest beam energy, therefore, those of higher energy beams become large.

The rms transverse beam sizes are shown in Fig. 9. To sufficiently suppress the beam size at lower beam energies,

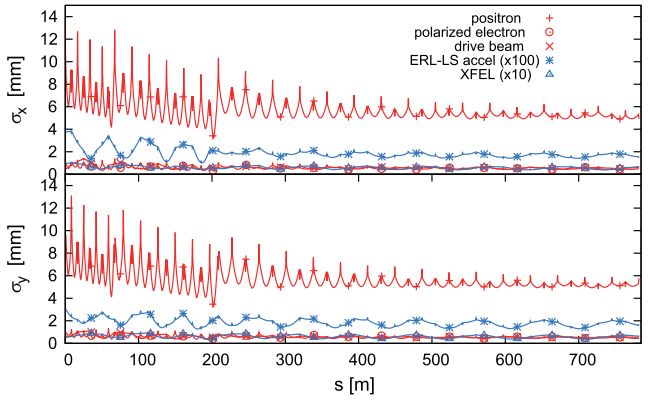

FIG. 9. Beam sizes in the horizontal (upper panel) and vertical (lower panel) directions of the long linac.

quadrupole triplets are inserted much more than a higher energy region. A quadrupole triplet is thus inserted after every two cavities at beam energies below 600 MeV, and after every four cavities at beam energies between 600 and 1300 MeV. At higher energies, they are inserted after every eight cavities. Therefore, the rms transverse size of the positron beam is focused to approximately 6 mm although adiabatic damping will shrink the actual size. Note that the quadrupole triplet allows transverse beam sizes above 6 mm because it operated at room temperature. Meanwhile, the rms transverse sizes of the electron beams for the XFEL and ERL-LS are maintained at less than 100 and 40 μm, respectively. Figure 10 shows the betatron functions. The betatron function of the decelerated beam of the ERL-LS, which loses energy in the downstream, must be maintained small; otherwise, the threshold beam current due to the HOM-BBU can be reduced. It is important to design the beam optics to restrain the betatron function of the decelerated beam with maintaining the rms transverse size of the positron beam small as described above. By virtue of this strategy, the betatron function of the ERL-LS is suppressed to within 120 m.

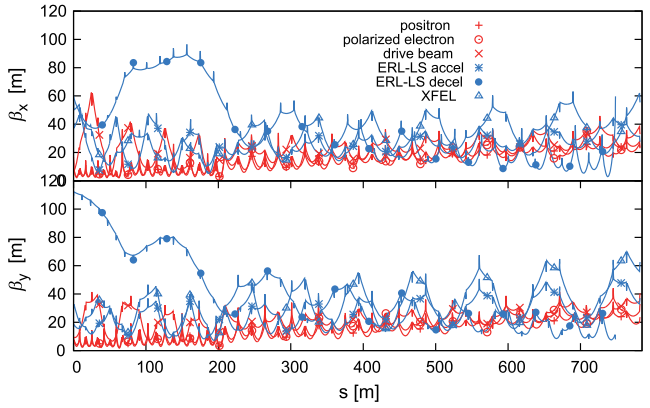

FIG. 10. Beta functions in the horizontal (upper panel) and vertical (lower panel) directions of the long linac.

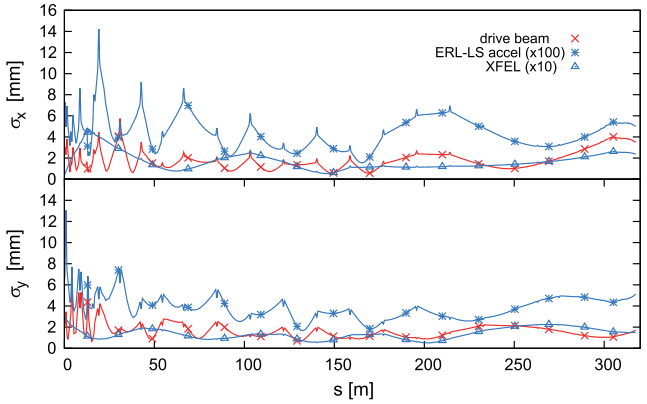

FIG. 11. Beam sizes in the horizontal (upper panel) and vertical (lower panel) directions of the short linac.

As the linac is divided into two main sections, no positrons pass through the short linac. Therefore, it is possible to optimize the beam optics for the ERL-LS, in which the maximum energy ratio between the accelerated and decelerated beams is high (almost 60), due to the injection and dump energy of 30 MeV and the full energy of 1.9 GeV. Some strategies are necessary to obtain reasonable optics without pulsed magnets. First, the linear optics is optimized for the lowest energy beam. Second, the beam optics are symmetrically designed over the entire short linac, because the energies of the accelerated and decelerated beam are symmetric. Next, the periodicity of the quadrupole triplet optics is slightly broken to maintain a small betatron function [38]. To further suppress the betatron function, the quadrupole triplets are installed between each cavity in the cryomodules in the low energy region. The betatron functions is calculated with 20 degree off-crest acceleration for the XFEL, and on-crest one for the ERL-LS. As shown in Fig. 11, the rms transverse beam sizes of the XFEL and ERL-LS are below 500 and 150 μm, respectively. If the emittance growth in the recirculation loop is negligible, the rms transverse sizes of the accelerated and decelerated beam are symmetric (data not shown).

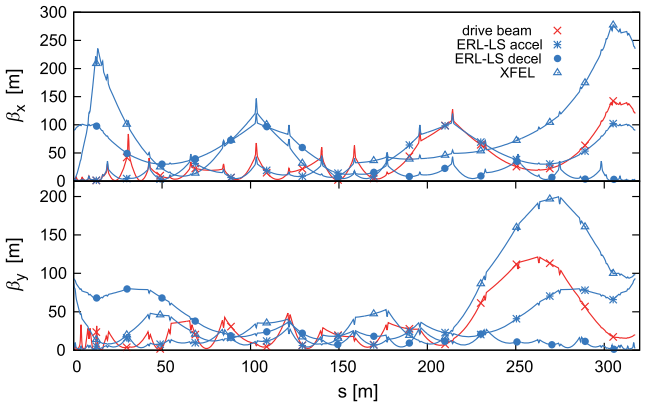

FIG. 12. Beta functions in the horizontal (upper panel) and vertical (lower panel) directions of the short linac.

The betatron function of the short linac is shown in Fig. 12. It can be suppressed lower than a few m in the cavity at the low energy region. According to our rough estimation, the threshold current due to HOM-BBU is slightly less than 100 mA. Therefore, the design value of the average electron beam current is 10 mA. In this estimate, the cavity type is assumed as the KEK-ERL model-1 cavity: that is the ILC nine-cell cavity equipped with enlarged beam pipes [31,34].

V. SUMMARY

In this article, we have proposed a shared SC linac as the ILC injector: polarized electron, positron, and their drive electron beams, and high-quality electron beams for the XFEL and ERL-LS as the x-ray light source. The electron beams for the light source are operated in the blank interval between the ILC pulses not to be affected by beam loading effects. Although each beam has a different energy, we have now designed reasonable linear optics for the linacs for the multibeam operation.

ACKNOWLEDGMENTS

I would like to express gratitude for fruitful discussions with Dr. M. Yamamoto and Professor K. Yokoya at KEK. I am also thankful for the comments of Dr. R. Hajima at National Institutes for Quantum and Radiological Science and Technology, and Professor M. Kuriki at Hiroshima University, and Dr. Si Chen at Shanghai Institute of Applied Physics.

[1] The International Linear Collider—Technical design report, 2013, https://ilchome.web.cern.ch/publications/ilc-technical-design-report.
[2] The European x-ray free-electron laser technical design report, DESY Report No. DESY 2006-097, 2007.
[3] LCLS-II conceptual design report, SLAC Report No. SLAC-R-1092, 2014.
[4] ESS technical design report, European Spallation Source Report No. ESS-doc-274, 2013.
[5] CLIC conceptual design report, CERN Report No. CERN-2012-007, 2013.
[6] M. Antonelli, M. Boscolo, R. Di Nardo, and P. Raimondi, Novel proposal for a low emittance muon beam using positron beam on target, Nucl. Instrum. Methods Phys. Res., Sect. A **807**, 101 (2016).
[7] F. Zimmermann, arXiv:1801.03170.
[8] M. Kuriki *et al.*, ILC positron source based on laser compton, AIP Conf. Proc. **980**, 92 (2008).
[9] M. Shimada *et al.*, in *Proceedings of the 4th International Particle Accelerator Conference, IPAC-2013, Shanghai, China, 2013* (JACoW, Geneva, Switzerland, 2013), p. 1598.

[10] T. Omori *et al.*, A conventional positron source for international linear collider, Nucl. Instrum. Methods Phys. Res., Sect. A **672**, 52 (2012).
[11] M. Kuriki *et al.*, in *Proceedings of LINAC2016, East Lansing, MI, USA* (JACoW, Geneva, Switzerland, 2017), p. 430.
[12] K. J. Kim, Y. Shvyd'ko, and S. Reiche, A Proposal for an X-Ray Free-Electron Laser Oscillator with an Energy-Recovery Linac, Phys. Rev. Lett. **100**, 244802 (2008).
[13] Energy Recovery Linac Conceptual Design Report, KEK Report No. 2012-4, 2012.
[14] Cornell energy recovery linac—Project definition design report, edited by G. Hoffstaetter, S. Gruner, and M. Tigner, Cornell University, 2012.
[15] R. Hajima, Energy recovery linacs for light sources, Rev. Accel. Sci. Techol. **03**, 121 (2010).
[16] M. Akemoto *et al.*, Construction and commissioning of the compact energy-recovery linac at KEK, Nucl. Instrum. Methods Phys. Res., Sect. A **877**, 197 (2018).
[17] M. Abo-Bakr *et al.*, in *Proceedings of the IPAC2017, Copenhagen, Denmark* (JACoW, Geneva, Switzerland, 2017), p. 855.
[18] R. Alarcon *et al.*, Transmission of Megawatt Relativistic Electron Beams through Millimeter Apertures, Phys. Rev. Lett. **111**, 164801 (2013).
[19] C. E. Reece, Continuous wave superconducting radio frequency electron linac for nuclear physics research, Phys. Rev. Accel. Beams **19**, 124801 (2016).
[20] D. Trbojevic *et al.*, in *Proceedings of the IPAC2017, Copenhagen, Denmark* (JACoW, Geneva, Switzerland, 2017), p. 1285.
[21] F. Méot *et al.*, in *Proceedings of the IPAC2016, Busan, Korea* (JACoW, Geneva, Switzerland, 2016), p. 1022.
[22] D. Angal-Kalinin*et al.*, PERLE: Powerful energy recovery linac for experiments—Conceptual design report, J. Phys. G **45**, 065003 (2018).
[23] M. Shimada *et al.*, in *Proceedings of the IPAC2016, Busan, Korea* (JACoW, Geneva, Switzerland, 2016), p. 3254.
[24] M. Shimada *et al.*, in *Proceedings of the 14th Annual Meeting of Particle Accelerator Society of Japan, Sapporo, Japan*, p. 781.
[25] Y. Ohnishi *et al.*, in *Proceedings of the 23rd International Linac Conference, LINAC-2006, Knoxville, TN, 2006* (JACoW, Geneva, Switzerland, 2006), p. 46.
[26] http://www-sldnt.slac.stanford.edu/alr/slc.htm.
[27] R. E. Laxdal *et al.*, in *Proceedings of the SRF2017, Lanzhou, China, 2006* (JACoW, Geneva, Switzerland, 2006), p. 6.
[28] N. G. Gavrilov *et al.*, Project of CW race-track microtron-recuperator for free-electron lasers, IEEE J. Quantum Electron. **27**, 2626 (1991).
[29] G. H. Hoffstaetter and I. V. Bazarov, Beam-breakup instability theory for energy recovery linacs, Phys. Rev. ST Accel. Beams **7**, 054401 (2004).
[30] S. Chen, S.-L. Huang, K.-X. Liu, J.-E. Chen, M. Shimada, and N. Nakamura, Beam breakup simulation study for a high energy ERL, Chin. Phys. C **39**, 017006 (2015).
[31] N. Nakamura *et al.*, in *Proceedings of the ERL15, Stony Brook, NY* (JACoW, Geneva, Switzerland, 2006), p. 4, ISBN 978-3-95450-183-0.
[32] C. D. Tennant, K. B. Beard, D. R. Douglas, K. C. Jordan, L. Merminga, E. G. Pozdeyev, and T. I. Smith, First observations and suppression of multipass, multibunch beam breakup in the Jefferson Laboratory free electron laser upgrade, Phys. Rev. ST Accel. Beams **8**, 074403 (2005).
[33] C. Tennant *et al.*, in *Proceedings of the ER2017, Geneva, Switzerland, 2017* (JACoW, Geneva, Switzerland, 2017), p. 45, DOI: 10.18429/JACoW-ERL2017-TUIACC001.
[34] H. Sakai *et al.*, in *Proceedings of the ERL07, Daresbury, UK, 2017* (JACoW, Geneva, Switzerland, 2017), p. 56.
[35] J. Gao, in *Proceedings of the Particle Accelerator Conference, Dallas, TX, 1995* (IEEE, New York, 1995), p. 1055.
[36] M. Omet, H. Hayano, A. Kuramoto, T. Matsumoto, S. Michizono, T. Miura, and F. Qiu, High-gradient near-quench-limit operation of superconducting Tesla-type cavities in scope of the International Linear Collider, Phys. Rev. ST Accel. Beams **17**, 072003 (2014).
[37] T. Schilcher, Ph.D. thesis, Universität Hamburg, 1998.
[38] I. V. Bazarov, G. A. Krafft, and L. Merminga, in *Proceedings of the Particle Accelerator Conference, Chicago, IL, 2001* (IEEE, New York, 2001), p. 3347.